

### Spatiotemporal double-phase hologram for complex-amplitude holographic displays

Journal:	<i>Chinese Optics Letters</i>
Manuscript ID	COL-20-0239.R1
Manuscript Type:	Original
Date Submitted by the Author:	n/a
Complete List of Authors:	Sui, Xiaomeng He, Zehao; Tsinghua University, Department of Precision Instruments; Zhang, Hao; Department of Precision Instrument Cao, Liangcai; Tsinghua University, Dept. of Precision Instrument Chu, Daping; University of Cambridge, Department of Engineering Jin, Guofan; Tsinghua University
Keywords:	Computer generated holography, complex amplitude hologram, double phase hologram, holographic display
Subject Category:	Holography

SCHOLARONE™  
Manuscripts

Manuscript ID: COL-20-0239

Title: Spatiotemporal double-phase hologram for complex-amplitude holographic displays

Authors: Xiaomeng Sui, Zehao He, Hao Zhang, Liangcai Cao, Daping Chu, Guofan Jin

May 8, 2019

Dear Prof. Yuqing Zhang,

On behalf of all co-authors, we are submitting the revised manuscript (COL-20-023). We would like to thank you for giving us the possibility to improve our manuscript. We are deeply grateful to the reviewers for their valuable comments and suggestions. We accepted all reviewers' suggestions and a revision has been carried out to take all of them into account. The point-by-point response to reviewers' comments is reported below and all changes are highlighted within the manuscript. We would be delighted if the revised manuscript can be considered for Chinese Optics Letters.

Best regards,

Xiaomeng Sui and Liangcai Cao

### **Response to Reviewer #1.**

This work proposed a method to generate complex-amplitude holograms. This approach is spatial-temporal multiplexing based on the double phase technique. It shows the four spatial-modified double-phase holograms in sequence in the time domain. This letter compares the results of the proposed spatiotemporal DPHs with those of a single-pixel and a single sub-DPH, respectively, in both simulation and experiment. The authors claim that the reconstructed image of their complex-amplitude hologram is without reducing the original image size and has better reconstruction performance.

**Response:** Thank you very much for your careful reading and your valuable comments.

The following comments are for the authors to improve their work:

- The authors mention that the proposed complex hologram can be fully reconstructed without down-sampling. I think the proposed method is still a down-sampling process to produce a complex-amplitude hologram. The reconstructed image is just composed of the reconstruction results of the four temporal DPHs.

**Response:** Thank you very much for the valuable comments. In the generation of sub-DPHs, a down-sampling operation is actually included as a compromise to the maintaining of image size. The temporal combination of four sub-DPHs is introduced to make up the loss in sampling to some extent.

The statements of "avoid sampling loss" has been revised as "suppressing sampling loss".

- As for the single-pixel method, what the pixel pitch of the single-pixel method? I have some doubts about the results of Figures 4 and 5. If it is a single pixel (a pitch of  $\alpha$  and  $\beta$  in the two dictions), then it is the full-resolution case. In comparison, even though the proposed method is temporal

1  
2  
3 multiplexing, it is still a quarter of the resolution. The reconstructed image of a low-resolution  
4 hologram, in general, has a poorer image quality than that of a high-resolution one.

5 **Response:** Thank you very much for your critical comments. In the single-pixel method, the pixel pitch  
6 is equal to that of the phase SLM. Two phase holograms are downsampled and then combined as one  
7 DPH. The rest of the two holograms are discarded. This is the reason of the information loss in the  
8 single-pixel method. In the proposed method, the pixel pitch is also equal to that of the phase SLM.  
9 Two phase holograms are downsampled and then combined as one DPH. The reconstruction quality is  
10 mainly determined by the interference of the four adjacent pixels. In the single-pixel method, the four  
11 adjacent pixels are from four different complex pixels. In the proposed method, the four adjacent pixels  
12 are from two different complex pixels. We have carefully checked the reconstruction quality between  
13 this two methods both in simulations and experiments. It is shown that in this case, the reconstruction  
14 quality of macro-pixel method is better because the information loss is less as to the interference  
15 between the four adjacent pixels from two different complex pixels. That is why we use the macro-  
16 pixel method rather than the single-pixel method.

17  
18  
19  
20  
21  
22  
23 • How do the authors simulate the proposed spatiotemporal DPH method? Please explain how do they  
24 do the simulation.

25 **Response:** Thank you very much for your comments. The spatiotemporal DPH method is the temporal  
26 multiplexing of four sub-DPHs. The four sub-DPHs are generated from the grouped complex field,  
27 which are modified into macro-pixel encoded DPHs. In the numerical reconstructions, each of sub-  
28 DPHs is filtered through the FFT (Fast Fourier Transform) and iFFT operation. The reconstructed object  
29 fields of sub-DPHs are calculated through the back propagation of the reconstructed complex wavefront.  
30 The final results of the numerical reconstruction for the spatiotemporal DPH method are the average  
31 value of the intensities of reconstructed objects.

32  
33  
34  
35  
36 • Is the object image (baboon) from a public image dataset (USC-SIPI Image Database)? If so, please  
37 cite a reference about the source of the image.

38 **Response:** Thank you very much for your question. Yes, it is. The source of the image is now mentioned  
39 in the manuscript and we have cited a reference of the source of the image.

40  
41  
42 • In page 3, Line 2, ... which is "idental" with that of the original field. It should be "identical".

43 **Response:** Thank you very much. The typo has been corrected.

44  
45  
46 • In page 3, Line 11, ... has a "vertial" profile .... Do you mean "vertical"?

47 **Response:** Thank you very much. The typo has been corrected.

## 48 49 50 51 **Response to Reviewer #2.**

52 Authors present an approach to encode complex-amplitude light waves with spatiotemporal double-  
53 phase holograms which combines several known techniques. Validity of proposed approach is  
54 supported with numerical simulation and optical experiments.

55 Overall quality of the paper is high, the only drawback I had noticed is that results of experiments on  
56 numerical reconstruction of test images are evaluated by magnitude of intensity fluctuations. It is not  
57  
58  
59  
60

1  
2  
3 very accurate parameter because a single peak leads to enormous increase in its value. It would be  
4 more accurate if standard deviation was used instead.

5  
6 **Response:** Thank you very much for your valuable comments. We appreciate your suggestion that the  
7 standard deviation should be considered to indicate the quality of the reconstructions in Figure 3. The  
8 standard deviation of the curves has been presented in the revised manuscript.  
9

10  
11 There are also several misprints in the text:

12 1. Ref. 3: J. M. Florence, R. D. Juday, "Full-complex spatial filtering with a phase mostly DMD"  
13 Prof. SPIE 1558 (1991)  
14 Should be Proc., not Prof.  
15

16 **Response:** Thank you very much. The typo has been corrected.  
17

18 2. P1 L28: quality using blazing gratings [9]  
19 Blazed gratings.  
20

21 **Response:** Thank you very much. The typo has been corrected.  
22

23 3. P3 L8-19: The high-intensity section of Fig. 3(b) fluctuates only by 36.2 in gray value and that of  
24 Fig. 3(f) fluctuates by 45.4 in gray value, respectively.  
25 I believe that figures 3 (a) and 3 (e) were actually meant.  
26

27 **Response:** Thank you very much. The redundant sentences in the main text have been removed.  
28  
29  
30  
31  
32  
33  
34  
35  
36  
37  
38  
39  
40  
41  
42  
43  
44  
45  
46  
47  
48  
49  
50  
51  
52  
53  
54  
55  
56  
57  
58  
59  
60

# Spatiotemporal double-phase hologram for complex-amplitude holographic displays

Xiaomeng Sui(隋晓萌),<sup>1</sup> Zehao He(何泽浩),<sup>1</sup> Hao Zhang(张浩),<sup>1</sup> Liangcai Cao(曹良才),<sup>1,\*</sup> Daping Chu(初大平)<sup>2,\*\*</sup> Guofan Jin(金国藩),<sup>1</sup>

<sup>1</sup>State Key Laboratory of Precision Measurement Technology and Instrument, Department of Precision Instruments, Tsinghua University, Beijing 100084, China

<sup>2</sup>Centre for Photonic Devices and Sensors, Department of Engineering, University of Cambridge, 9 JJ Thomson Avenue, Cambridge CB3 0FA, UK

\*Corresponding author: [clc@tsinghua.edu.cn](mailto:clc@tsinghua.edu.cn); \*\* corresponding author: [dpc31@cam.ac.uk](mailto:dpc31@cam.ac.uk)

Received Month X, XXXX; accepted Month X, XXXX; posted online Month X, XXXX

This letter describes an approach to encode complex-amplitude light waves with spatiotemporal double-phase holograms (DPHs) for overcoming the limit of the space-bandwidth product (SBP) delivered by existing methods. To construct DPHs, two spatially macro-pixel encoded phase components are employed in the SBP-preserved resampling of complex holograms. Four generated sub-DPHs are displayed sequentially in time for high-quality holographic image reconstruction without reducing the image size or discarding any image terms when the DPHs are interweaved. The reconstructed holographic images contain more details and less speckle noise, with their signal-to-noise ratio and structure similarity index being improved by 14.64% and 78.79%, respectively.

**Keywords:** Computer generated holography, complex amplitude hologram, double phase hologram, holographic display  
doi:10.3788/COLXXXXX.XXXXXX.

Using conventional spatial light modulators (SLMs) for complex modulation of coherent light beams is a challenging task. Because current SLMs cannot perform full complex modulation on a single panel, the complex holograms generated by computers must be converted into amplitude-only holograms or phase-only holograms. In 1970, Lee decomposed a two-dimensional complex field into two functions with a constant amplitude in conjunction with different spatially distributed phase functions [1]. The complex field was then retrieved through the coherent superposition of the two waves. In 1978, Hsueh and Sawchuk used phase functions to generate double-phase holograms (DPHs) for binary devices [2]. In these methods, two phase-only patterns are encoded into a single phase hologram by using combined sub-cells to produce the desired complex field.

DPHs have attracted significant attention because they can be implemented using phase-only SLMs, such as liquid crystal SLMs [3-4]. In 2002, Arrizón modified a double-phase holographic code to be used through phase-only SLMs without increasing the complexity of hologram cells [5-7]. Since a pixelated complex field uses doubled or quadrupled number of phase-only pixels on the SLM, which can only modulate a complex hologram with a half or quarter of its resolution. In 2014, Mendoza-Yero et al. used binary gratings to sample phase elements and combined them with a  $4-f$  optical system to synthesize complex fields [8]. This method allows for single-pixel operation without an array of subpixels for codifying each pixel in an input plane. It maintains the same image size as that of the original image, but results in a sampling loss.

Various attempts based on the single-pixel on-axis DPH configuration have been made, to improve the image quality using **blazed gratings** [9] and realize complex modulation for three-dimensional scenes [10]. In 2019, a DPH method with a weight factor was introduced to reduce the peripheral noise and expand the SBP for DPHs [11], in which the weight factor is multiplied by an amplitude and used to modify the phase function for reducing the noise in image peripherals and extending expressible areas.

In the traditional digital encoding methods, two phases can hardly be interweaved completely into a DPH, whose size is identical to that of an original complex field, without information loss. In this work, we propose a spatiotemporal encoded DPH to **suppress information loss** by using multiple resampled sub-DPHs together with time multiplexing which can reduce speckles and expand viewing zones in holographic displays [12-16]. Such a spatiotemporal multiplexing method combines spatial coding and temporal coding to achieve high-quality image reconstructions with the proposed DPHs, without reducing image sizes or losing any terms of complex fields.

From Fig. 1(a), it is clear that the  $(i, j)^{\text{th}}$  pixel value of a pixelated complex hologram  $u(x, y)$  can be expressed by its amplitude and phase as  $u_n^{i,j} = A^{i,j} \exp(i\phi^{i,j})$ , where  $i$  and  $j$  are the pixel indices. The pixels of the complex hologram  $u_h(x, y)$  are then divided into four groups  $u_1(x, y)$ ,  $u_2(x, y)$ ,  $u_3(x, y)$  and  $u_4(x, y)$  consisting of non-adjacent pixels. The neighbors of every pixel in each group are excluded from the same group. Therefore, it is convenient to transform pixels in a group into macro-pixels formed by arrays of  $2 \times 2$  phase-only pixels, as is shown in Fig. 2.

We assume that the desired complex field is encoded by a phase-only SLM with rectangular pixels having a rectangular pixel-active window with dimensions of  $a \times b$  and pixel distances of  $\alpha$  and  $\beta$ . The rectangular functions that represent the SLM pixels and complex macro-pixels are defined as

$$\omega_h(x, y) = \text{rect}(x/a)\text{rect}(y/b), \quad (1)$$

$$\omega_c(x, y) = \text{rect}(x/2\alpha)\text{rect}(y/2\beta). \quad (2)$$

The complex wavefront of the group  $u_1(x, y)$  modulated by a spatially quantized element can be expressed as [5]

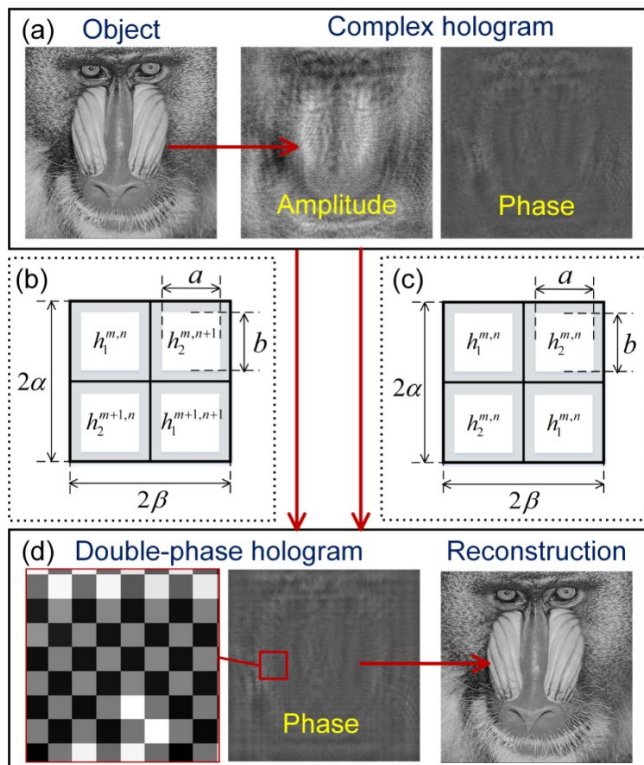


Fig. 1. Processing procedure for a DPH. (a) Transformation of an original object into its complex hologram. (b) Encoding principle for the single-pixel method. (c) Encoding principle for the macro-pixel method. (d) DPH encoded by the macro-pixel method.

$$u_1(x, y) = \sum_{m,n} u_1^{m,n} \omega_c(x - 2n\alpha, y - 2m\beta), \quad (3)$$

where  $u_1^{m,n} = A^{m,n} \exp(i\phi^{m,n})$  is the  $(m, n)^{\text{th}}$  pixel value of  $u_1(x, y)$ . By assuming that  $u$  and  $v$  are spatial frequencies, the desired reconstruction of a complex hologram can be obtained by applying a Fourier transform and bandwidth limiting as

$$U_1(u, v) = p(u, v) \sum_{m,n} u_1^{m,n} \exp[-i2\pi(2n\alpha u, 2m\beta v)] \quad (4)$$

where  $p(u, v) = 4\alpha\beta \text{sinc}(2\alpha u) \text{sinc}(2\beta v)$  is the bandwidth-limited function.

To obtain the encoded complex field, every pixel in the complex hologram is transformed into a macro-pixel by

using an array of  $2 \times 2$  phase-only pixels to perform complex decomposition (Fig. 1(b)). The decomposed phase functions are

$$h_1^{m,n} = \exp(\phi^{m,n} - \Delta^{m,n}), \quad (5)$$

$$h_2^{m,n} = \exp(\phi^{m,n} + \Delta^{m,n}), \quad (6)$$

where the phase shift is  $\Delta^{m,n} = \cos^{-1}(A^{m,n})$ . Knowing that

$$h_{\text{sub1}}(x, y) = \sum_{m,n} h^{m,n}(x, y),$$

we refer to other transformed groups of pixels into sub-DPHs  $h_{\text{sub2}}(x, y)$ ,  $h_{\text{sub3}}(x, y)$  and  $h_{\text{sub4}}(x, y)$ , each of which contains only 1/4 information in the complex hologram, but has the same size as the complex hologram.

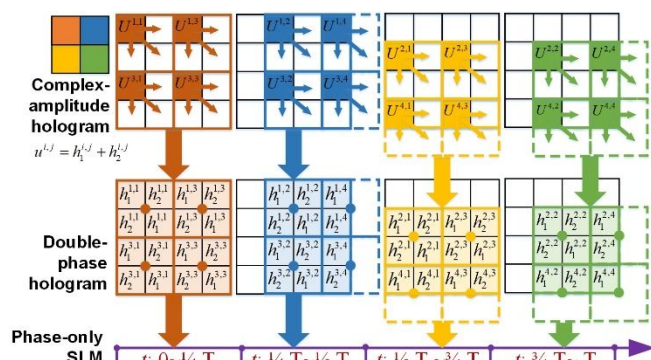


Fig. 2. Decomposition of a complex hologram into four sub-holograms and time-sequential uploading onto an SLM in the proposed spatiotemporal multiplexing method.

The sub-DPHs are sequentially uploaded onto a phase-only SLM and reconstructed on the back focal plane of a  $4f$  system. The SLM should be equipped with a high frame rate to ensure the sub-DPHs are played at an adequately short time interval, so that all the macro-pixels from sub-DPHs are combined for time-sequential display which is captured by human eyes or detectors. Thus the complex hologram can be fully reconstructed without down-sampling.

The reconstructed image from the sub-DPH  $h_{\text{sub1}}(x, y)$  encoded by the macro-pixels can be expressed by [5]

$$H_1(u, v) = p_S(u, v) \sum_{m,n} \begin{pmatrix} \cos(\Delta^{m,n}) \exp(i\phi^{m,n}) g \\ \exp[-i2\pi(2n\alpha u + 2m\beta v)] \end{pmatrix} + p_N(u, v) \sum_{m,n} \begin{pmatrix} \sin(\Delta^{m,n}) \exp(i\phi^{m,n}) g \\ \exp[-i2\pi(2n\alpha u + 2m\beta v)] \end{pmatrix}, \quad (7)$$

where  $p_S(u, v)$  and  $p_N(u, v)$  donate the following bandwidth-limited functions,

$$p_S(u, v) = 4ab \cos(\pi\alpha u) g \cos(\pi\beta v) \text{sinc}(\alpha u) \text{sinc}(\beta v), \quad (8)$$

$$p_N(u, v) = -i4ab \sin(\pi\alpha u) g \sin(\pi\beta v) \text{sinc}(\alpha u) \text{sinc}(\beta v). \quad (9)$$



$H_i(u, v)$  consists of a signal term which is identical with that of the original field, and a noise term generated by the spatial shifts between the two different phases that encode the complex field. The quality of reconstruction largely depends on the bandwidth-limited functions  $p_s(u, v)$  and  $p_N(u, v)$ . The cosine factors of signal function  $p_s(u, v)$  restrict the hologram signal field to the on-axis centered square band with dimensions of  $\Delta u = 1/\alpha$  and  $\Delta v = 1/\beta$ . The noise function  $p_N(u, v)$  has a vertical profile that is null along the axes of  $u=0$  and  $v=0$ . It should be noted that the maximum value of  $p_N(u, v)$  occurs along the axes of  $u = v$  and  $u = -v$ . To block high-noise areas in the spectrum plane, a filter is introduced usually in reconstruction.

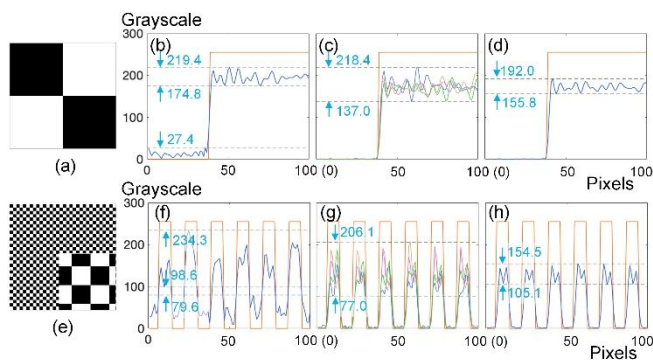


Fig. 3. Numerical reconstructions of test images using different methods. (a) Original amplitude with mostly low-spatial-frequency components. (b) Reconstruction of (a) using a single-pixel DPH. (c) Reconstructions of (a) using sub-DPHs. (d) Reconstruction of (a) using spatiotemporal multiplexing DPHs. (e) Original amplitude with mostly high-spatial-frequency components. (f) Reconstruction of (e) using a single-pixel DPH. (g) Reconstructions of (e) using sub-DPHs. (h) Reconstruction of (e) using spatiotemporal multiplexing DPHs. The red curves represent the original image and other colored curves represent the reconstructed images.

But the interweaving of two functions makes it unavoidable to allow part of the noise to pass through and lose part of the signal, resulting in reconstruction noise or signal loss. Since the factor  $\sin(\Delta^{m,n}) \exp(i\phi^{m,n})$  varies with different sub-DPHs, impacts of the noise term are weakened by time-averaging of four sub-DPHs. A bandlimit by the requisite filter in the Fourier plane is eased and the available bandwidth is thus expanded.

To illustrate the working principles of the proposed spatiotemporal multiplexing method, two test images with the same constant phase but different amplitudes are considered. One has mostly low-spatial-frequency components (Fig. 3(a)) and the other has mostly high-spatial-frequency components (Fig. 3(e)). Each image was encoded using a single-pixel DPH, four separated sub-DPHs and a spatiotemporal multiplexing DPH, respectively. The images reconstructed from single-pixel

DPH (Figs. 3(b) and 3(f)) contain ground noises up to 79.6 in gray value. The standard deviation for high-intensity section of Fig. 3(b) is 11.36 in gray value and that of Fig. 3(f) is 37.73 in gray value. They have inaccurate edges and details, indicating the loss of high-spatial-frequency components. In the reconstructions based on sub-DPHs (Figs. 3(c) and 3(g)), the ground noise is alleviated by macro-pixel encoding to almost null. In the high-intensity sections of the images, there are major distortions, representing complementary shapes among the four reconstructions. When time encoding is introduced to coordinate macro-pixel encoding, intensity multiplication enhances the contrast in the image to an accurate level. The standard deviation for high-intensity section of Fig. 3(d) is 7.10 in gray value and that of Fig. 3(h) is 32.57 in gray value.

Figure 4 presents the numerical reconstruction of a complex hologram with an image size of  $512 \times 512$  pixels, which is generated from an original image in USC-SIPI Image Database [17]. The image reconstructed by the spatiotemporal multiplexing DPH method (Fig. 4(d)) includes more details and less noise than the image reconstructed by the single-pixel DPH method (Fig. 4(b)). It also has a much higher peak signal-to-noise ratio (PSNR) of 21.21 dB and structure similarity index (SSIM) of 0.59, while the single-pixel method yields an image with a PSNR of 18.50 dB and SSIM of 0.33. It indicates a 14.64% increase in PSNR and a 78.79% increase in SSIM, respectively. The parameter of filter has impacts on the image quality. Curves of PSNRs and SSIMs for the reconstructed images changing with the diameter of filter are provided in Fig. 4(e) and Fig. 4(f), respectively. These improvements show that the image reconstructed by the spatiotemporal multiplexing DPH method is much closer to the original image in terms of very minute details. The image reconstructed by one of the four sub-DPHs without time encoding (Fig. 4(c)) also shows improved performance in terms of noise suppression compared to the single-pixel method.

To demonstrate the effectiveness of the proposed spatiotemporal multiplexing method experimentally, we implemented the optical setup as shown in Fig. 5. A coherent beam at  $\lambda=532$  nm is emitted from a solid-state laser acting as a light source. It is then attenuated and expanded before passing through a polarizer and onto a reflective liquid crystal on silicon (LCoS) phase-only SLM (Holoeye Gaya). The SLM has a pixel number of  $3840 \times 2160$ , pixel pitch of  $3.74 \mu\text{m}$ , and frame rate of 60 Hz. The desired complex hologram is decomposed and encoded into four sub-DPHs  $h_{\text{sub}1}(x, y)$ ,  $h_{\text{sub}2}(x, y)$ ,  $h_{\text{sub}3}(x, y)$ , and  $h_{\text{sub}4}(x, y)$ , which are then time-sequentially uploaded onto the SLM at a rate of 60 Hz. The beam splitter (BS) allows for both the plane wave illuminating onto the SLM as well as the reflection towards a 4-f system with a filter to block unwanted diffraction orders.

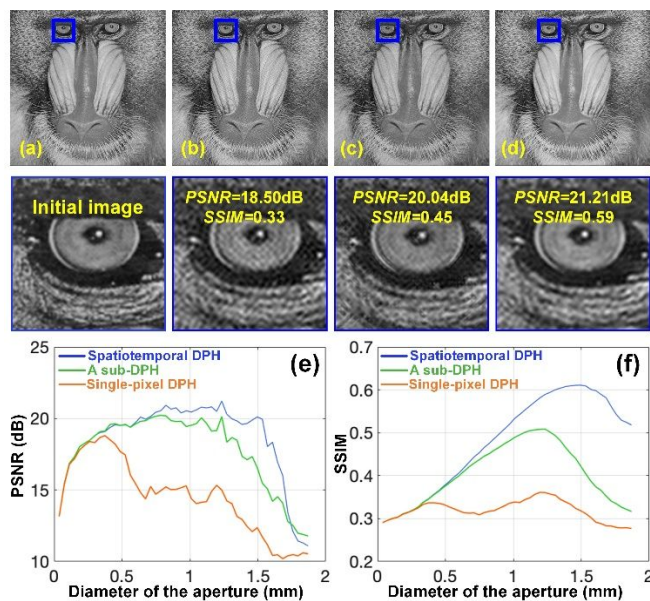


Fig. 4. Numerically reconstructed images based on different methods. (a) Original image. (b) Reconstruction using a single-pixel DPH. (c) Reconstruction using one sub-DPH. (d) Reconstruction using spatiotemporal multiplexing DPHs. (e) Curves of PSNRs for the reconstructed images changing with the diameter of filter. (f) Curves of SSIMs for the reconstructed images changing with the diameter of filter.

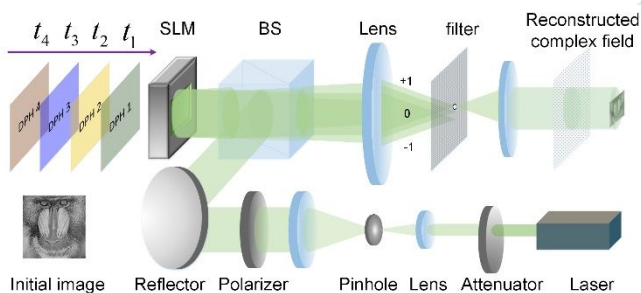


Fig. 5. Schematic of the optical system for the proposed DPH method.

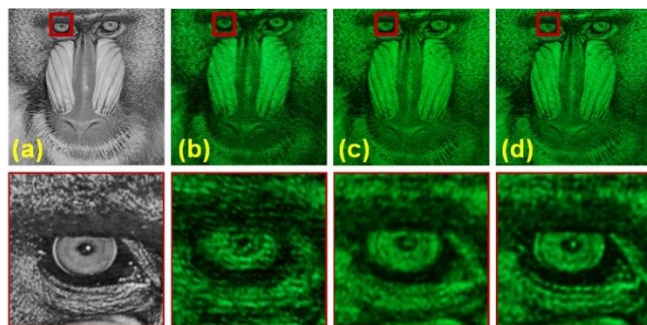


Fig. 6. Optically reconstructed images using different methods with partial enlargement. (a) Original image. (b) Reconstruction using a single-pixel DPH. (c) Reconstruction using one sub-DPH. (d) Reconstruction using a spatiotemporal multiplexing DPH.

Figure 6 shows the optically reconstructed images captured by using a CMOS detector. It can be seen that the image reconstructed by the spatiotemporal multiplexing DPH method (Fig. 6(d)) retains most its original features. Compared to the single-pixel method (Fig. 6(b)), it preserves the edges and most details of the image with much less blurring and noise. It has the PSNR of 11.44 dB and SSIM of 0.18, while the image reconstructed by the single-pixel method has only PSNR of 11.30 dB and SSIM of 0.14, respectively.

In summary, the proposed spatiotemporal multiplexing DPH method can deliver high quality images through SBP-preserved resampling and increased time-bandwidth product. It improves the capability of DPHs to preserve the details of reconstructed images and suppresses the information loss during hologram interweaving. This makes the spatiotemporal DPHs a suitable method for the digital modulation of both static and quasi-static complex fields with existing SLMs. It can be used in a wide range of applications based on complex holograms, from high quality holographic display to optical field generation.

**Funding.** National Science Foundation of China (NSFC) projects (61827825, 61775117) and Tsinghua University Initiative Scientific Research Program (20193080075).

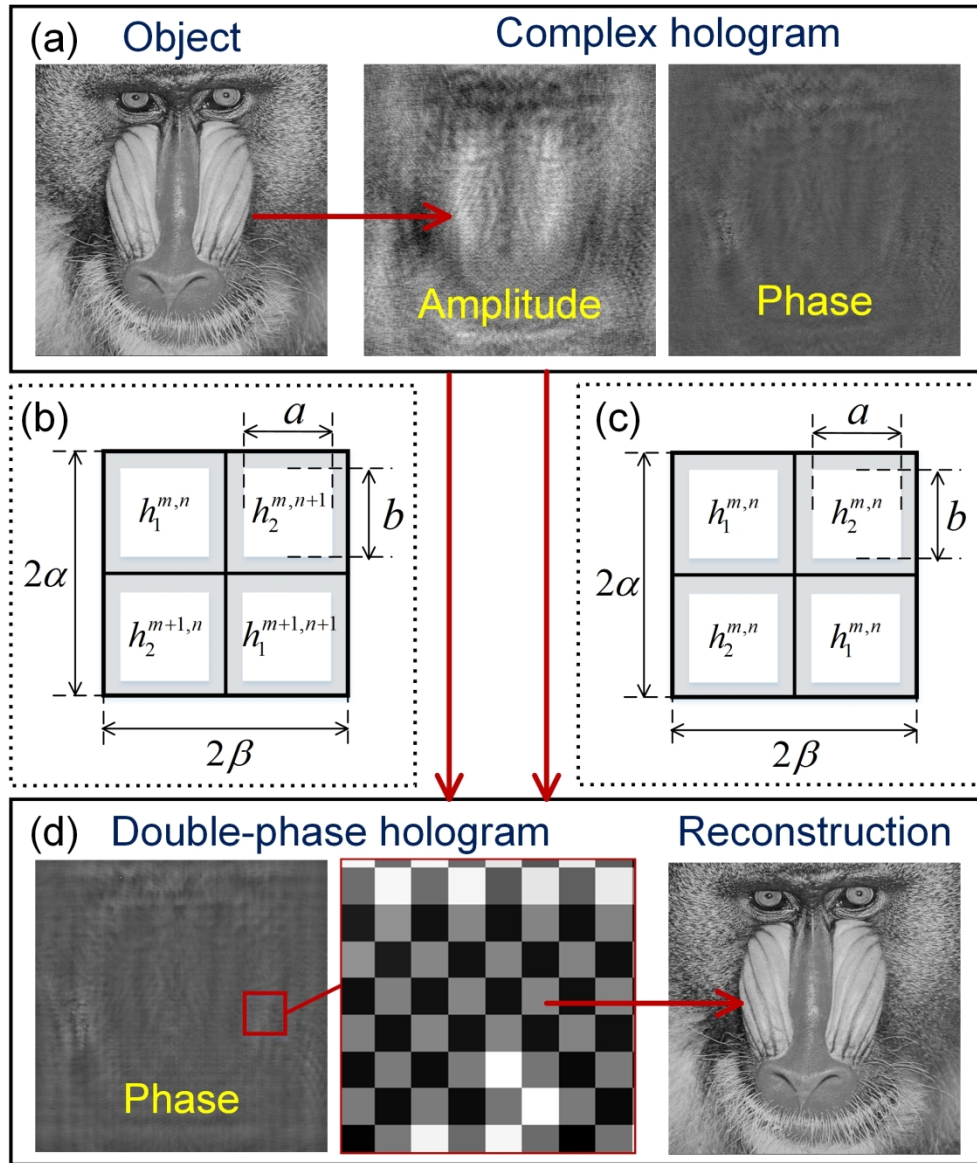
## References

- W. H. Lee, *Appl. Opt.* **9**, 639 (1970).
- C. K. Hsueh and A. A. Sawchuk, *Appl. Opt.* **17**, 3874 (1978).
- J. M. Florence and R. D. Juday, *Proc. SPIE* **1558** (1991)
- D. Mendlovic, S. Gal, L. Uriel, Z. Zeev, and M. Emanuel, *Appl. Opt.* **36**, 8427 (1997).
- V. Arrizon, *Opt. Lett.* **27**, 595 (2002).
- V. Arrizon and D. Sanchez-de-la-Llave, *Appl. Opt.* **41**, 3436 (2002).
- V. Arrizón, *Opt. Lett.* **28**, 2521 (2003).
- Mendoza-Yero, G. Mínguez-Vega, and J. Lancis, *Opt. Lett.* **39**, 1740 (2014).
- Y. J. Qi, C. L. Chang, and J. Xia, *Opt. Express* **24**, 30368 (2016).
- D. Z. Kong, L. C. Cao, G. F. Jin, and B. Javidi, *Appl. Opt.* **55**, 8296 (2016).
- Y. K. Kim, J. S. Lee, and Y. H. Won, *Opt. Lett.* **4**, 3649 (2019).
- Y. Takaki and M. Yokouchi, *Opt. Express* **19**, 7567 (2011).
- Y. Sando, D. Barada, and T. Yatagai, *Opt. Lett.* **39**, 555 (2014).
- Y. Takaki and K. Fujii, *Opt. Express* **22**, 24713 (2014).
- Y. Zhao, L. C. Cao, H. Zhang, W. Tan, S. H. Wu, Z. Wang, Q. Yang, and G. F. Jin, *Chinese Opt. Lett.* **14**, 5 (2016).
- S. Ikawa, N. Takada, H. Araki, H. Niwase, H. Sannomiya, H. Nakayama, M. Oikawa, Y. Mori, T. Shimobaba, T. Ito, *Chinese Opt. Lett.* **18**, 1 (2020)
- A. G. Weber, *USC-SIPI Rep.* **315**, 1 (1997).

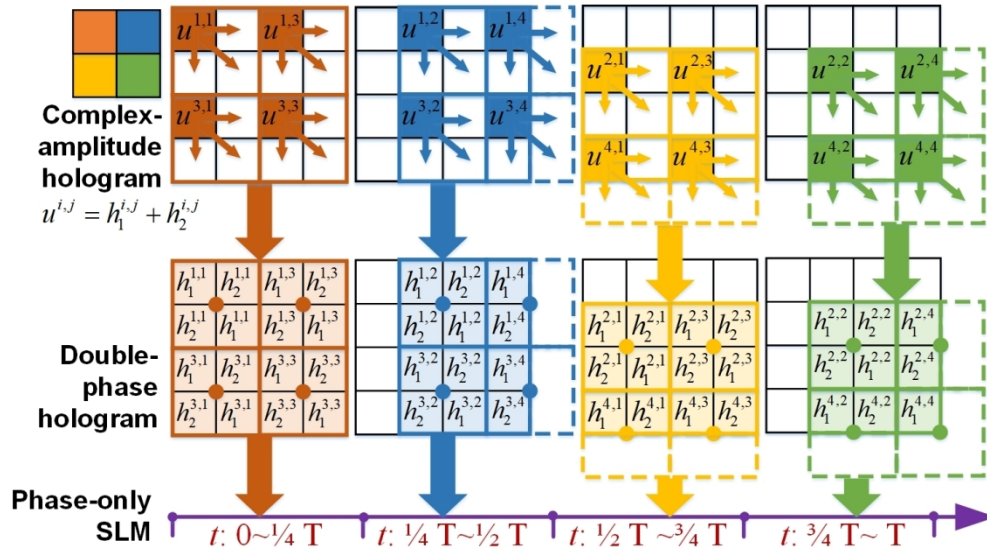


## References for review

1. W. H. Lee, "Sampled Fourier transform hologram generated by computer." *Applied Optics* **9**, 639 (1970).
2. C. K. Hsueh, A. A. Sawchuk, "Computer-generated double-phase holograms" *Applied Optics* **17**, 3874 (1978).
3. J. M. Florence, R. D. Juday, "Full-complex spatial filtering with a phase mostly DMD" *Proc. SPIE* **1558** (1991)
4. D. Mendlovic, S. Gal, L. Uriel, Z. Zeev, M. Emanuel, "Encoding technique for design of zero-order (on-axis) Fraunhofer computer-generated holograms." *Applied Optics* **36**, 8427 (1997).
5. V. Arrizon, "Improved double-phase computer-generated holograms implemented with phase-modulation devices." *Optics Letters* **27**, 595 (2002).
6. V. Arrizon, D. Sanchez-de-la-Llave, "Double-phase holograms implemented with phase-only spatial light modulators: performance evaluation and improvement." *Applied Optics* **41**, 3436 (2002).
7. V. Arrizón, "Optimum on-axis computer-generated hologram encoded into low-resolution phase-modulation devices." *Optics Letters* **28**, 2521 (2003).
8. Mendoza-Yero, G. Mínguez-Vega, and J. Lancis, "Encoding complex fields by using a phase-only optical element." *Optics Letters* **39**, 1740 (2014).
9. Y. J. Qi, C. L. Chang, J. Xia. "Speckleless holographic display by complex modulation based on double-phase method." *Optics Express* **24**, 30368 (2016).
10. D. Z. Kong, L. C. Cao, G. F. Jin, B. Javidi, "Three-dimensional scene encryption and display based on computer-generated holograms." *Applied Optics* **55**, 8296 (2016).
11. Y. K. Kim, J. S. Lee, Y. H. Won, "Low-noise high-efficiency double-phase hologram by multiplying a weight factor." *Optics Letters* **4**, 3649 (2019).
12. Y. Takaki, M. Yokouchi, "Speckle-free and grayscale hologram reconstruction using time-multiplexing technique." *Optics Express* **19**, 7567 (2011).
13. Y. Sando, D. Barada, T. Yatagai, "Holographic 3D display observable for multiple simultaneous viewers from all horizontal directions by using a time division method." *Optics Letters* **39**, 555 (2014).
14. Y. Takaki, K. Fujii, "Viewing-zone scanning holographic display using a MEMS spatial light modulator." *Optics Express* **22**, 24713 (2014).
15. Y. Zhao, L. C. Cao, H. Zhang, W. Tan, S. H. Wu, Z. Wang, Q. Yang, G. F. Jin, "Time-division multiplexing holographic display using angular-spectrum layer-oriented method." *Chinese Optics Letters* **14**, 5 (2016).
16. S. Ikawa, N. Takada, H. Araki, H. Niwase, H. Sannomiya, H. Nakayama, M. Oikawa, Y. Mori, T. Shimobaba, T. Ito, "Real-time color holographic video reconstruction using multiple-graphics processing unit cluster acceleration and three spatial light modulators." *Chinese Optics Letters* **18**, 1 (2020)
17. A. G. Weber, "The USC-SIPI image database version 5," *USC-SIPI Report* **315**, 1 (1997).

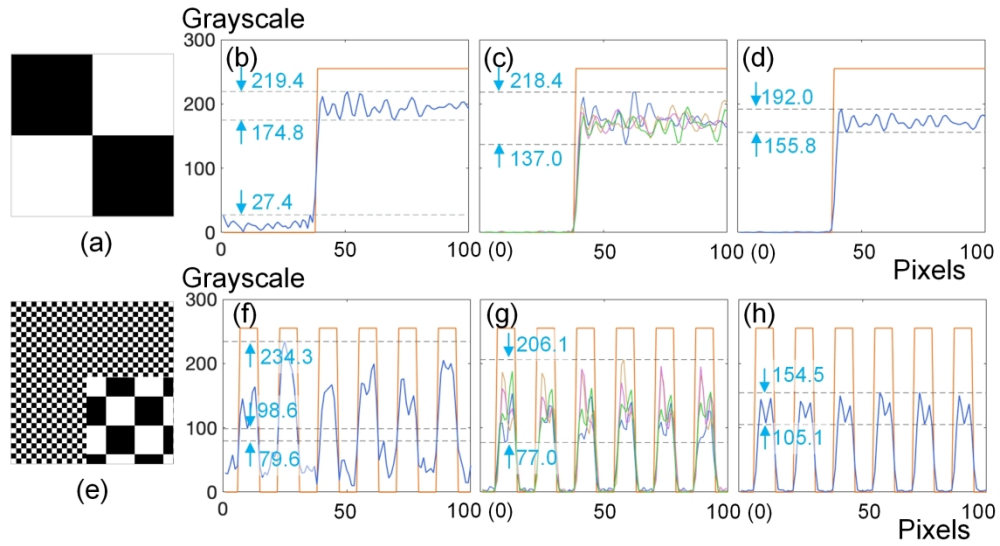


205x239mm (300 x 300 DPI)



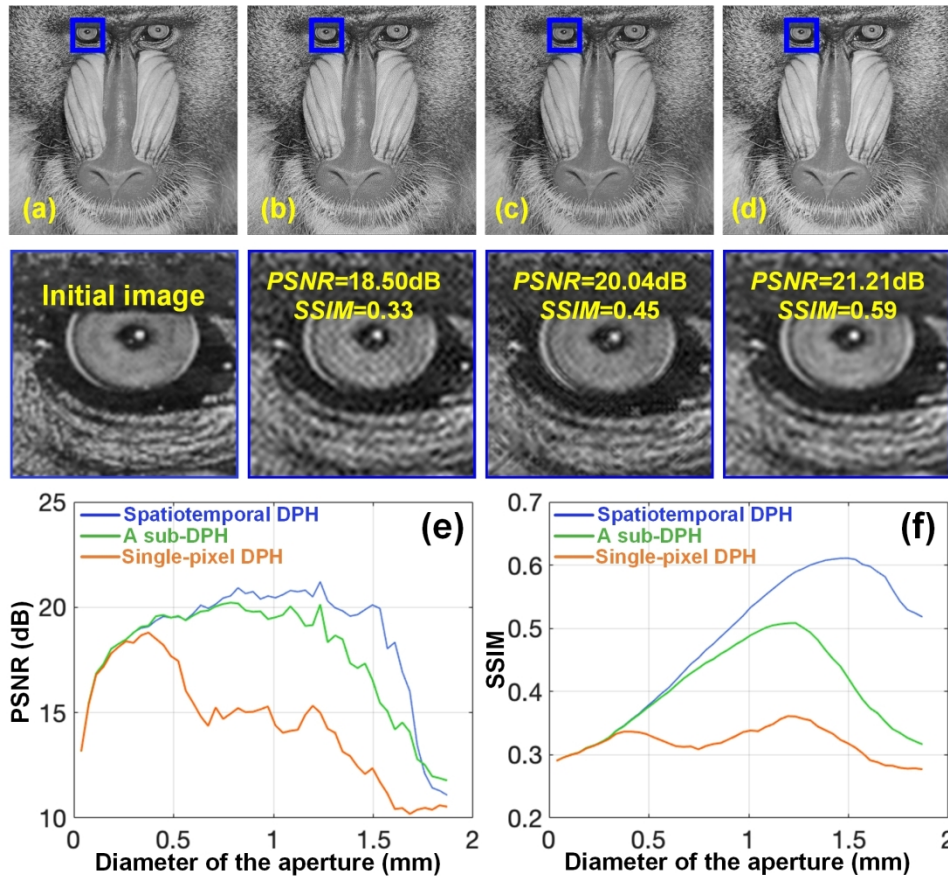
321x182mm (120 x 120 DPI)

1  
2  
3  
4  
5  
6  
7  
8  
9  
10  
11  
12  
13  
14  
15  
16  
17  
18  
19  
20  
21  
22  
23  
24  
25  
26  
27  
28  
29  
30  
31  
32  
33  
34  
35  
36  
37  
38  
39  
40  
41  
42  
43  
44  
45  
46  
47  
48  
49  
50  
51  
52  
53  
54  
55  
56  
57  
58  
59  
60

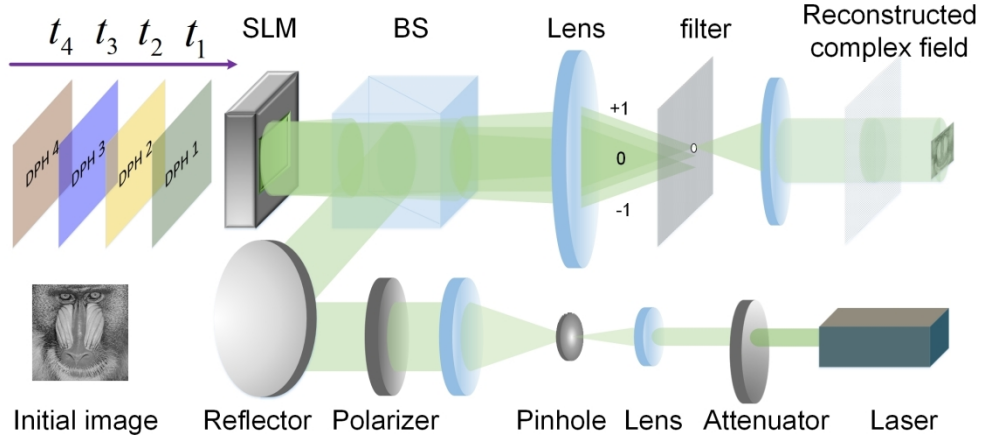


231x135mm (300 x 300 DPI)



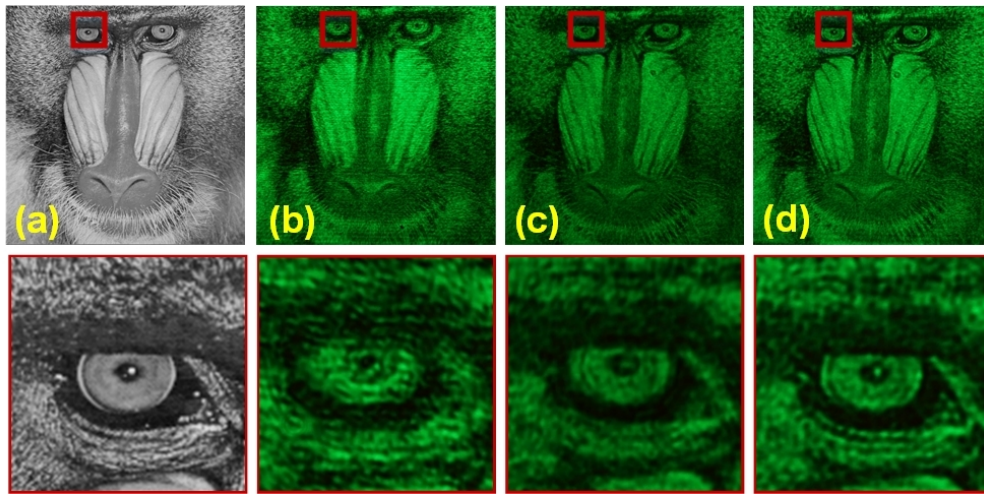


174x153mm (300 x 300 DPI)



466x212mm (120 x 120 DPI)

1  
2  
3  
4  
5  
6  
7  
8  
9  
10  
11  
12  
13  
14  
15  
16  
17  
18  
19  
20  
21  
22  
23  
24  
25  
26  
27  
28  
29  
30  
31  
32  
33  
34  
35  
36  
37  
38  
39  
40  
41  
42  
43  
44  
45  
46  
47  
48  
49  
50  
51  
52  
53  
54  
55  
56  
57  
58  
59  
60



166x81mm (150 x 150 DPI)